2.5 REPLACING THE MEYERS ET AL. FORMULA IN BULK ICE MICROPHYSICS SCHEMES IN CANADIAN MESOSCALE MODELS

Faisal S. Boudala* and George A. Isaac

Cloud Physics and Severe Weather Research Section, Environment Canada, Toronto, Ontario, Canada

1. INTRODUCTION

Ice clouds in the atmosphere are very important in that they strongly affect the earth's radiation balance and hydrological cycle (*Liou* 1986; *Stephens et al*. 1990). They can exist both at high and lower altitudes, but their initiation and formation mechanisms are not well understood. There are two types of nucleation modes for producing ice particles in clouds depending on temperature. At temperatures ($T > -40^oC$), ice particles are produced as a result of heterogeneous nucleation in the presence of small insoluble aerosol particles that serve as ice nuclei. At temperatures ($T < -40^oC$), however, supercooled liquid drops may freeze instantaneously and become ice particles and this is normally referred to as homogeneous nucleation (*Pruppacher and Klett* 1997).

It is believed that there are at least four different modes of heterogeneous nucleation such as contact, immersion, deposition, and condensation freezing depending on how the liquid droplets and water vapor interact with the aerosol particles (see *Pruppacher and Klett* 1997 for more discussions). However, it is not clear which modes are more relevant to natural atmospheric ice particle production. The observed ice concentration in clouds often exceeds the measured ice nucleus concentration by several order of magnitude (e.g. *Gultepe et al.* 2001), and this has been attributed to the fact that the ice concentration may also be enhanced due to secondary ice multiplication mechanisms such as break up during collusion (*Vardiman* 1976) or shattering and splintering during riming (*Hallett and Mossop* 1978). However, many of the current Numerical Weather Prediction (NWP) and General Circulation models (GCM) cloud ice microphysics schemes including those used in the UK Met-Office Unified Model (*Wilson and Ballard* 1999), the ARCSCM (*Morrison et al*. 2003), the CSIRO GCM(*Rotstayn* 1997), and the Canadian Mesoscale Compressible Community (MC2) model (*Benoit et al*. 1997) use diagnostic parameterizations for ice nuclei number concentrations based on *Fletcher* (1962), *Meyers et al.* (1992) or *Cooper* (1986). The bulk ice microphysics schemes used by various models vary slightly, but generally follow similar methods. For simplicity, in this paper, we will focus on the *Kong and Yau* (1997) microphysics scheme (KY from here on). This scheme has been implemented in the Canadian MC2 model. In this scheme, there are several processes such as ice nucleation, ice deposition/sublimation, melting, riming, and sedimentation. The total ice particle concentration is estimated based on the *Meyers et al.* (1992) formula and the ice particles are assumed to be spherical with a density of pure ice.

Tremblay et al. (2001) found that the KY scheme overestimates the cloud top pressure and the amount of low level clouds. Tremblay et al. have suggested that this is probably caused by an unrealistically high terminal velocity for ice particles used in the model. *Ryan et al.* (2000) have compared several models including MC2 with the KY scheme against satellite and ICCP data, and found that all the models simulated excess cirrus clouds as compared to the mid-level clouds. They hypnotized that this is the result of ice sublimation in the model that suppresses the development of mid-level clouds. *Guan et al.* (2002) also found that KY scheme overestimates the number of glaciated clouds as compared to the in-situ aircraft observations. Thus, as will be discussed later, these discrepancies in model predictions may also be associated with the use of a formula provided by *Meyers et al.* (1992) for predicting the ice concentration, particularly at cold temperatures. The recent ARCSCM simulation by *Morrison et al*. (2005) using both Meyers et al. and Cooper's equations for specification of ice nucleus concentration in the model also shows that the model predicts significantly less liquid water at cold temperatures ($T<-23\ ^oC$) as compared to observations during SHEBA. Nonetheless, there are no detailed studies of ice microphysics in the KY scheme against observations. The aim of this paper is to test the validity of using the

* *Corresponding author address*: Faisal S. Boudala
Cloud Physics and Severe Weather Research Section, Environment Canada, Toronto, Ontario, Canada, M3H 5T4
E-mail: faisal.boudala@ec.gc.ca.

ice nucleus concentration given by *Meyers et al.* (1992) (Meyers from now on) and the assumption of spherical ice particles in the KY scheme. For this purpose, in-situ aircraft measurements taken during several field projects in extra tropical regions will be used, and finally a new ice microphysics scheme will be presented.

2. IN-SITU OBSERVATIONS

2.1 *Field Projects*

The data were collected during four projects using the National Research Council (NRC) Convair-580 aircraft. The Beaufort and Arctic Storms Experiment (BASE) field project was conducted in October 1994 over the Canadian Western Arctic near the Beaufort Sea and other (*Gultepe et al.* 2000). The FIRE Arctic Cloud Experiment (FIRE.ACE) project began in April 1998 and ended in July 1998, with the Convair-580 measurements being made in April. The main objectives of FIRE.ACE were to study the impact of Arctic clouds on the radiation exchange between the surface and the atmosphere (*Curry et al.* 2000). The Canadian Freezing Drizzle Experiment I (CFDE I) project was carried out in March 1995 over Newfoundland and the Atlantic Ocean. The Canadian Freezing Drizzle Experiment III (CFDE III) started in December 1997 and ended in February 1998. During CFDE III project, the aircraft flew over Southern Ontario and Quebec, Lake Ontario and Lake Erie. These two projects were aimed at studying aircraft icing in winter storms, but a significant portion of the clouds encountered were glaciated (*Isaac et al*. 2001; *Cober et al.* 2001).

2.1 Instrumentation

The types of instrumentation used in these projects are described in *Isaac et al.* (2001). The calibrations of the instruments and processing of the data are described in *Cober et al.* (2001). The instruments used for in this work are the PMS FSSP, 2D-C, 2D-P probes (*Knollenberg* 1981, 1970), the Nevzorov liquid water content (LWC) and total water content (TWC) probes, and LiCor Li-6262 water vapor analyzer for measuring the relative humidity.

The Nevzorov TWC/LWC probe is discussed in detail by *Korolev et al*. (1998b). The probe has two separate sensors, one for total water content (TWC) and the other for liquid water content (LWC) measurements. Comparison measurements made with Nevzorov and similar types of probes in high speed wind tunnel experiments suggests that the probe can measure LWC and TWC within an accuracy of 15% and the sensitivity of the instrument is estimated to be in the range of 0.003 to 0.005 gm^{-3}. However, there are some uncertainties about the collection efficiency of this instrument.

The Forward Scattering Spectrometer Probe (FSSP) was designed to measure sizes and concentrations of spherical particles. An earlier study by *Gardiner and Hallett* (1985) indicated that the FSSP measured ice concentration was 2-3 orders of magnitude higher than those derived from a replicator, but later *Arnott et al.* (2000) showed that the replicator under estimates concentrations of particles (D<50μm). The more recent study by *Field et al*. (2003) suggests that the FSSP probe may overestimate ice concentration on average by a factor of 2 due to shattering of ice particles on the tip of the probe.

The PMS 2D-C and 2D-P probes measure concentrations in the particle size ranges of 25 – 800 μm and 200 – 6400 μm respectively. However, the first 4 channels (25-100 μm) of the 2D-C have been ignored here because of measurement uncertainty. The identification of ice clouds follows the *Cober et al.* (2001) scheme. Based on this scheme, the stratiform ice clouds are characterized by an FSSP concentration < 15 cm^{-3}, a Rosemount icing detector < 2 mVs^{-1}, and the Nevzorov LWC/TWC ratio <0.25. The temperature has been measured with a Rosemount temperature probe and the minimum temperature measured was near -40°C. In this paper, for all calculations, 30s (approximately 3km) averaged data have been used.

The detailed description and calibration of the LiCor Li-6262 water vapor analyzer are given in LiCor (1996). This instrument estimates the ambient water vapor concentration by measuring the attenuation of IR radiation crossing a sampling volume. The instrument is calibrated using known amounts of water vapor produced from a dew point generator or measured using a hygrometer. The accuracy of this instrument depends on both the calibration methods and other factors. The manufacturer's calibration provides water vapor pressure measurements with an uncertainty of close to 1%.

3. ICE PARTICLE MASS AND TEMINAL VELOCITY

3.1 The Ice Particle Size Distribution

In most models, the ice particle size distribution is represented by a generalized gamma distribution function as

$$N_i(D_i) = N_{io} D_i^{k} \exp(-\lambda_i D_i) \quad (1)$$

where the coefficients λ_i, N_{io}, and k are the slope, intercept, and dispersion coefficients. However, these

coefficients are not generally well known and at least two of the variables have to be known in order to calculate the other. There are several ways of estimating these coefficients. In some models, both ice mixing ratio q_i and the ice concentration are predicted and then the coefficients are related to moments of the ice particle spectra. This scheme is referred to as the double moments scheme (e.g. *Ferrier et al.* 1995) and requires significant computer power and has some computational problems in separating the advection fields of the mass and number concentration. In this paper, we will focus on the single moment KY scheme. In this scheme, q_i is provided by the model and if one assumes ice particles are spheres with a density of pure ice, the ice mixing ratio (q_i) can be related to the size distribution of ice particles as

$$q_i = \frac{\rho_i \pi}{6\rho} \int_0^\infty D_i^3 N_i(D_i) dD_i = \frac{\rho_i \pi N_{io}}{6\rho} \frac{\Gamma(4+k)}{\lambda_i^{4+k}} \qquad (2)$$

where ρ is the air density, ρ_i is the ice density, and Γ is a gamma function. It is possible to calculate the slope parameter from Eq. 2 in terms of the intercept and dispersion parameters, but these quantities are unknown. In the KY scheme, the dispersion parameter is assumed to be zero, thus only the intercept parameter has to be known. This was achieved by calculating the total concentration N_t as

$$N_t = \int_0^\infty N_t(D_i) dD_i = \frac{N_{io}\Gamma(1+k)}{\lambda_i^{1+K}}. \qquad (3)$$

It is now possible to solve for N_{io} from Eq. 3 and inserting the expression in Eq. 2 provides a solution for λ_i as

$$\lambda_i = \left[\frac{\pi \rho_i N_t \Gamma(4+k)}{6\rho q_i \Gamma(1+k)} \right]^{1/3}. \qquad (4)$$

However, Eq. 4 can only be helpful if the total ice particle concentration is known. To circumvent this problem KY use the Meyers formula for total ice particle concentration as

$$N_m = \exp(k_1 + k_2 S_i), \qquad (5)$$

where k_1 and k_2 are some constants, and S_i the ice supersaturation predicted by the model. At this point, both the slope and intercept parameters are known. From now on, the slope parameter λ_i given in Eq. 4 with N_m will be referred to as λ_{KY}, the intercept parameter as N_{oKY}, the ice mixing ratio as q_{KY}. However, the formula given in Eq. 5 was developed based on surface measurement of ice forming nuclei using a continuous diffusion chamber in Sierra Nevada. *Meyers et al.* (1992) have indicated that this formula can only be used for a temperature range -7 ^{o}C to -20 ^{o}C, and an ice supersaturation S_i range of 2% to 25%, and it may not be applicable for other geographical locations. However, as discussed earlier, ice particle number concentration in the natural clouds can also be enhanced due to the secondary ice multiplication mechanisms such as shattering and splintering other than just nucleation alone. Furthermore, the use of this formula is also limited by the difficulty of determining the ice supersaturation in a given model.

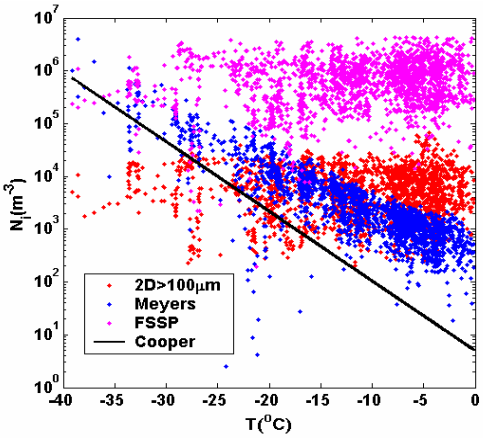

Figure 1. Ice concentration versus temperature estimated using the Meyers and Cooper's formulas, and as measured with the 2D-C and 2D-P probes for D > 100 μm. probes, and the FSSP probe.

As will be discussed later, these parameters are used to estimate very important meteorological phenomena such as precipitation, nucleation, melting and riming and thus should be known within a reasonable accuracy. Figure 1 (panel 1) shows ice particle concentrations plotted against temperature using measurements from the two dimensional (2D) optical array probes (2D-C and 2D-P) (D_i>100 μm) and estimates using Eq. 5 based on measured S_i. The formula that is given in Eq. 5 overestimates (underestimates) the concentration at cold (warm) temperatures as compared to 2D measurements. Also shown in the same figure are the small ice particle (D_i <100 μm) concentrations measured using the FSSP probe for comparisons. Although this probe is believed to overestimate the concentration of small ice particles, on average it could be trusted within a factor of two uncertainty (*Field et al.* 2003). Note that for temperatures colder than -35^{o}C (for cirrus type clouds), the Meyers's formula would give ice concentrations even much higher than that would be measured with the FSSP probe. This may partly explain the *Ryan et al.* (2000) findings discussed earlier. The parameterization

of N_i as a function of temperature based on limited aircraft measurements (*Cooper* 19886) is also shown in the figure for comparison. The ice concentration calculated based on the Cooper's parameterization under estimates the concentration by several order of magnitude as compared to the 2D measurements, at cold temperatures, but it is comparable to the Meyers formula. This may explain why *Morrison et al.* (2005) found very little liquid water at cold temperatures. The main conclusions reached from Fig. 1 are similar to those found by *Gultepe et al*. (2001). Therefore, it is more appropriate to use a parameterization of the size distribution of ice particles instead of the concentration for application in bulk ice microphysics schemes as has been done in KY and other schemes. This will be discussed in section 5.

Figure 2 shows the ratios derived N_{oKY} to observed N_{io} (panel a), λ_{KY} to observed λ_i (panel b), and concentration estimated from observed λ_i and N_{io} plotted against temperature using the 2D-C and 2D-P measurements assuming an exponential size distribution. Similar to concentration, these parameters are overestimated (underestimated) at colder (warmer) temperatures. It is not obvious in Fig. 2, but as will be shown later in section 5, both the intercept and slope parameters on average increase with decreasing temperatures and this is consistent with the trends reported by *Heymsfield et al.* (2002).

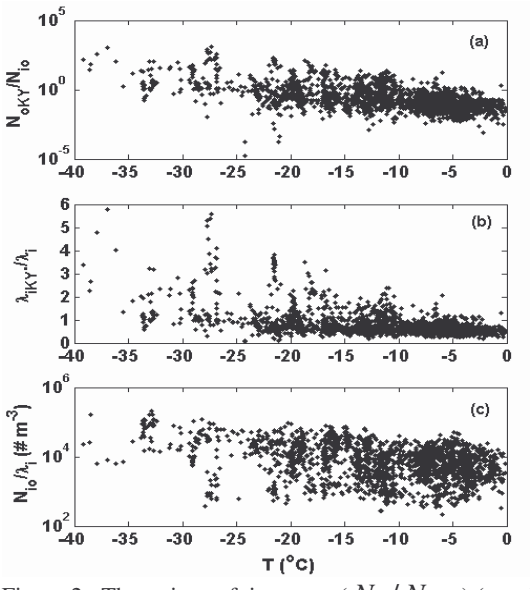

Figure 2. The rations of intercept (N_{io}/N_{oKY}) (panel a) and slope (λ_{KY}/λ_i) parameters (panel b), of the ice particle size distributions estimated from the KY scheme and observations, and the ratio (N_{io}/λ_i) based on observations (panel c) are plotted against the measured cloud temperature.

From Eq. 3, it can be seen that the total concentration increases with increasing N_{io}, but decreases with increasing λ_i. The net effect on ice concentration (ratio N_{oKY}/λ_i) as shown in Fig. 2 (c) is to diminish the temperature dependence of ice concentration. This is also consistent with the measured ice concentration shown in Fig. 1. This may partly explain why measured ice concentration has a weak temperature dependence. Thus, the total concentration of ice particles for a given temperature is determined by these two opposing processes. Therefore, it is more appropriate to use a parameterization of the size distribution of ice particles instead of the concentration for application in bulk ice microphysics schemes as has been done in KY and other schemes. This will be discussed in section 5.

3.2 Ice Particle Mass And Terminal Velocity

Ice particles in the natural atmosphere are not necessarily spherical in shape (*Korolev et al.* 2000). Their densities are not well known and may vary anywhere from a few g cm^{-3} to about 0.92 g cm^{-3} for pure ice. The spherical shape assumption, particularly when the density of pure ice is used as has been done in the KY scheme, severely overestimates the ice mass (see Fig. 3). Therefore, to avoid this problem, it is customary to use experimental mass to size relationship in a form

$$m(D_i) = dD_i^c \tag{6}$$

where m is a mass in grams of a single particle with size D_i, and d and c are some constants. In this paper, the coefficients are set as c =2.25 and d =205.548 gm^{-c} and where D_i is given in m following *Heymsfield* (2003). Although, the coefficients c and d depend on particle shape (habit), it is possible to assume that ice particles are irregular in shape (aggregates) since about 80% of can be categorized as irregular shape (*Korolev et al.* 2000). Figure 3 also shows the comparisons of ice mixing ratio derived using the *Heymsfield* (2003) mass size relationship against measurements obtained using the Nevzorov probe during several aircraft field projects. Although, there are some discrepancies at lower ice mixing ratios, within measurement uncertainty, the agreement between derived and measured is quite reasonable.

Similarly, there are expressions also for ice particle terminal velocity in a form

$$\upsilon_i = aD_i^b \left(\frac{\rho_o}{\rho}\right)^{1/2}, \tag{7}$$

where a and b are constants and ρ_o is the reference air density and the coefficients a =4.836 $m^{(-b+1)}$ s^{-1} and b =0.25 are the same as in the KY scheme, where D_i in m.

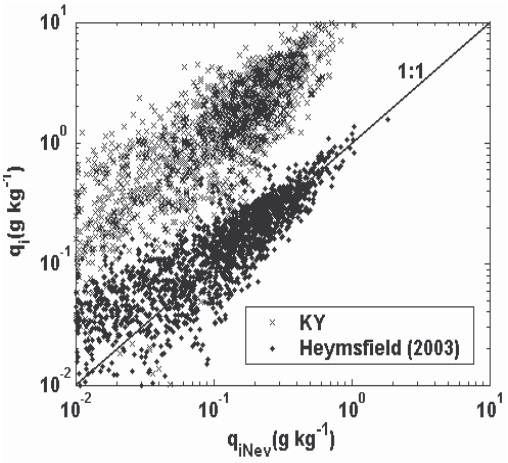

Figure 3. The ice mixing ratios estimated using the KY scheme (ice spheres), and the Heymsfield (2003) coefficients, are plotted the measured mixing ratio using Nevzorov probe.

4. BULK ICE MICROPHYSICS

The mass weighted terminal velocity can be derived as

$$V_i = \frac{\int_0^\infty \upsilon_i(D_i) m_i(D_i) N_i(D_i) dD_i}{\int_0^\infty m_i(D_i) N_i(D_i) dD_i} \tag{8}$$

We propose to use Eqs. 7 and 8 and the solution is

$$V_i = \left(\frac{\rho_o}{\rho}\right)^{1/2} \frac{a\Gamma(k+b+c+1)}{\Gamma(k+c+1)\lambda_i^b} \tag{9}$$

In the KY scheme, c = 3 instead of 2.25 as in this work and the slope parameter λ_i derived using the KY scheme would be represented as λ_{KY} .

Figure. 4 shows the ratio (V_{KY}/V_i) of mass weighted terminal velocity calculated using the KY scheme (assuming that ice particles are spheres with density of pure ice for mass calculations) and the observed ice spectrum and Heymsfield's coefficients (panel a). The ratio of the ice mass flux (KY/Ob) is also shown (panel b). The KY scheme, generally overestimates the mean fall velocity at warmer temperatures except at temperatures (T<-25°C) where the KY scheme slightly underestimates the fall velocity. The overestimation of V_i mainly comes about because λ_{KY} is smaller than the observed λ_i at warmer temperatures. The downward flux of ice depends on both the vertical distribution ice mass and the mass weighted terminal velocity. Although, there are some uncertainties about the ice particle mass in the new scheme, as seen from Fig. 3, Heymsfield's coefficients gave a more realistic mass than the original KY scheme, and thus the KY scheme is probably unrealistically high. Thus as shown in Fig. 4 (panel b), the mass flux calculated using the KY scheme is larger than the one calculated using the Heymsfield's coefficients. This is consistent with the finding of *Tremblay et al.* (2001) that the KY scheme over predicted the cirrus cloud top pressure level, which suggests possible overestimation of the ice sedimentation rate or terminal velocity. Although significant numbers of ice particles are being generated at cold temperatures due to the Meyers formula, the removal process may also be enhanced for some temperatures as discussed earlier.

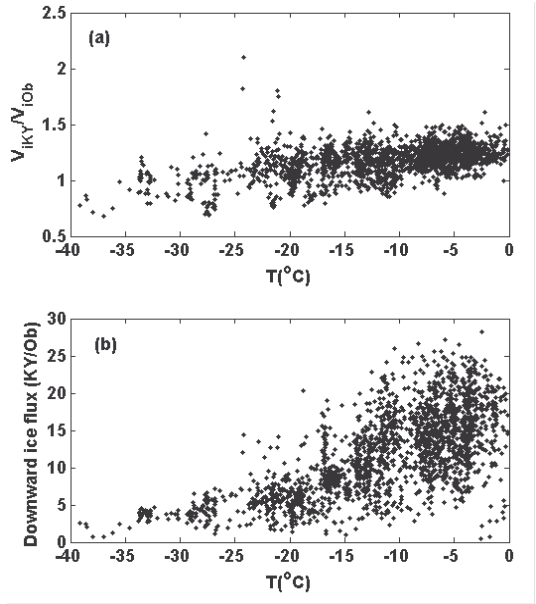

Figure 4. The ratio of the mass weighted terminal velocity estimated KY scheme (ice spheres) and the observation of ice spectrum (a), and ratio of mass flux ($(q_{iKY} * V_{iKY})/(q_i * V_i)$) (b).

4.2 Ice Vapor Deposition And Riming

Ice deposition and sublimation of ice particles (VD_{vi}) can be derived following KY as

$$VD_{vi} = \frac{1}{\rho}\int_0^\infty \frac{dm_i}{dt} N_i(D_i) dD_i \tag{10a}$$

where

$$\left(\frac{dm_i}{dt}\right)_{VD} = \frac{2\pi D_i S_i f(\mathrm{Re})}{G_i} - \frac{L_s L_f}{K R_w T^2 G_i}\left(\frac{dm_i}{dt}\right)_{rim}, \qquad (10b)$$

K is the thermal conductivity of air, R_w is the specific gas constant of vapor, L_s is the latent heat of sublimation and L_f is the latent heat of fusion. The ventilation factor is given as $f(\mathrm{Re}) = 1 + 0.23\,\mathrm{Re}^{1/2}$, where Re is the Reynolds 's number given by as $\mathrm{Re} = (D_i v_i)/\nu$, where ν is the kinematic viscosity of air, and G_i is a thermodynamic quantity defined as

$$G_i = \frac{L_s^2}{K R_w T} + \frac{R_w T}{D_f e_{is}}, \qquad (10c)$$

where T is temperature, e_{is} is the saturation vapor pressure over ice, and D_f is the vapor diffusion coefficient. The

$$\left(\frac{dm_i}{dt}\right)_{rim} = \frac{\pi D_i^2}{4} v_i(D_i) E_{ic} \rho q_c \qquad (10d)$$

where E_{ic} the collection efficiency and q_c is the liquid water mixing ratio. The solution is given as

$$VD_{vi} = \frac{2\pi S_i N_{io}}{G_i}\left(\frac{\Gamma(2+k)}{\lambda^{k+2}} + 0.23\left(\frac{a}{\nu}\right)^{1/2}\left(\frac{\rho_o}{\rho}\right)^{1/4}\frac{\Gamma(2.5+0.5b+k)}{\lambda^{2.5+0.5b+k}}\right) - \frac{L_f \pi a E_{ic} q_c N_{io}}{4 K R_w T^2 G_i}\left(\frac{\rho_o}{\rho}\right)^{1/2}\frac{\Gamma(b+3+k)}{\lambda^{b+3+k}} \qquad (10e)$$

The only difference between Eq. 10e and the original KY scheme is that the coefficients N_{oKY} and λ_{KY} would have been used.

Figure 5 (panel a) shows the ratio of ice deposition rate calculated using the KY scheme and based on observed spectra for an assumed liquid mixing ratio of 0.00004 kg kg^{-1}. The KY scheme generally overestimates the ice deposition rate at colder temperatures and underestimates at warmer temperatures following the trend in ice concentration shown earlier. Since the KY scheme is applied for much colder atmospheric conditions, such as cold cirrus, it is possible that too much ice could be produced at much colder temperatures (T<-25^{o}C).

The ice growth rate by riming is given by an expression as

$$CL_{ci} = \frac{1}{\rho}\int_0^\infty \left(\frac{dm_i}{dt}\right)_{rim} N_i(D_i) dD_i \qquad (11e)$$

The solution is given as

$$CL_{ci} = \frac{\pi a E_{ic} q_c N_{io}}{4}\left(\frac{\rho_o}{\rho}\right)^{1/2}\frac{\Gamma(b+3+k)}{\lambda_i^{b+3+k}} \qquad (11b)$$

Figure 5 (panel b) shows the ratio of riming calculated using the KY scheme and the same assumed liquid water mixing ratio used in panel a and measured spectra. On average, the KY scheme overestimates (underestimates) the riming rate at colder (warmer) temperatures, but not as much as in the ice deposition case shown in panel a. Since the riming rate has a relatively stronger size dependence than the ice deposition rate, the effect of the ice concentration calculated using the Meyers formula has relatively weaker effects on riming as compared to ice deposition. The riming rate calculated using the KY scheme also shows very little temperature dependence as compared to the observations, which show a general increase in riming with increasing temperature as would be expected.

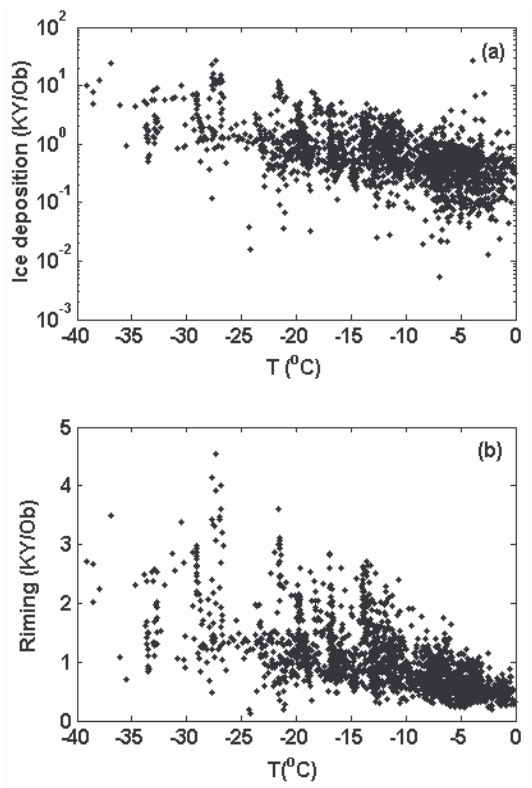

Figure 5. The ratios of ice deposition (a) and riming (b) rates calculated from KY scheme, and observed spectra are plotted against temperature.

5. THE PARAMETERIZATION OF N_{io} AND λ_i

The need for the Meyers formula in the bulk microphysics schemes is mainly due to the fact that the ice particle size distribution is not well known and other

alternatives were unavailable. The parameterization of N_{io} and λ_i follows *Boudala* (2004).

Figure 6 shows the observed N_{io} (panel a) and λ_i (panel b) discussed earlier are plotted against the total ice water content derived using the Heymsfield's coefficients for ice particles sizes (D>100 um) and the mass of small ice particles ($D_i \leq 100$ µm) are estimated following *Boudala et al.* (2002). Generally the contribution of the small ice particles to the total mass on average is less than 20% (*Boudala et al.* 2002), thus if ignored may not make significant difference. However, it is included here for consistency since the model predicted ice mass is usually assumed to include all particle sizes although they may not be specified in the model. For a given q_i, both λ_i and N_{io} increase with decreasing temperature. The physical interpretation of decreasing λ_i with increasing temperature suggests increasing aggregation with increasing temperature, and increasing N_{io} with decreasing temperature implied the production of small ice particles.

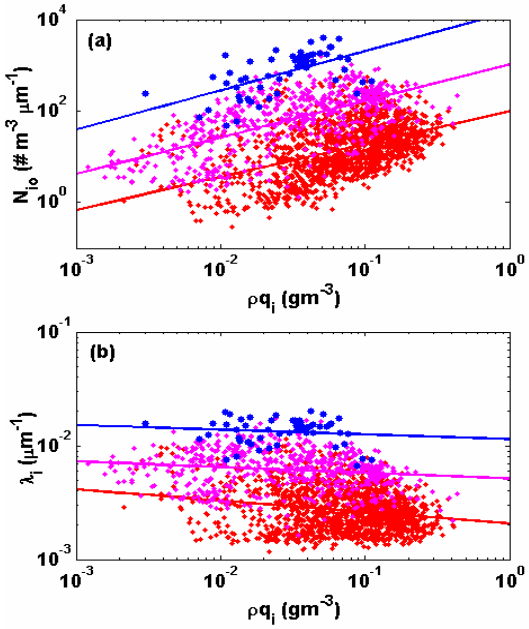

Figure 6. The measured intercept (a) and slope (b) parameters are plotted ice water content derived using Heymisfield's coefficients and the best fit lines for shown temperature intervals are shown.

For a given temperature, λ_i (N_{io}) increases (decrease) with decreasing q_i, which suggests that increasing q_i is associated with an increase in both small ice particle production and ice particle growth via vapor deposition and aggregation processes. Based on Fig. 6, power law relationships are derived as

$$N_{io} = n_{oa}(T)(\rho q_i)^{n_{ob}(T)}$$
$$\lambda_i = \lambda_a(T)(\rho q_i)^{\lambda_b(T)} \quad , \qquad (12a)$$

where ρ is the density of air, the coefficients $\lambda_a(T)$, $\lambda_b(T)$, $n_{oa}(T)$, and $n_{ob}(T)$ are related to temperature as given in Fig 7. Each point in the figure represents the median values of the observed N_{io}, λ_i and temperature (T) for the temperature intervals shown in Fig. 6. The mean square fits for these coefficients are given as

$$n_{oa} = a_1 \exp(b_1 T)$$
$$n_{ob} = c_1 T + d_1 \qquad (12b)$$

$$\lambda_a = a_2 \exp(b_2 T)$$
$$\lambda_b = c_2 T + d_2 \qquad (12c)$$

where T is the cloud temperature in °C, and a_1, a_2, b_1, b_2, c_1, c_2, d_1 and d_2 are constants given in Table 1. The intercept parameter N_{io} is given in m^{-3}µm^{-1} and λ_i is in µm^{-1}. The dispersion parameter k is set to zero.

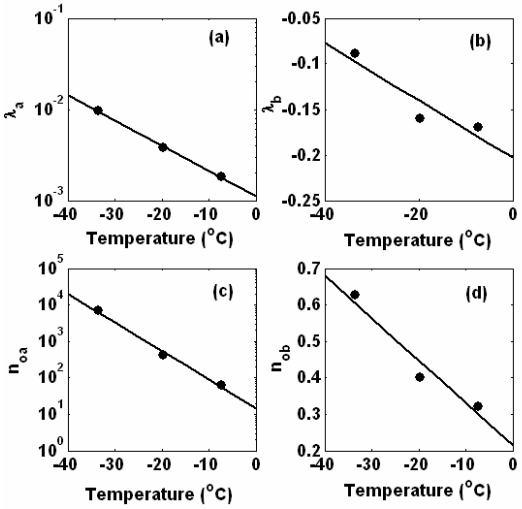

7. The coefficients in Eqs. 12a and 12b are related to temperature and the best fit lines are also given (see Eqs. 12b and 12c).

The size distribution of small particles is not well known. Studies suggest that the distribution of particles may be parameterized using a gamma distribution function (*Boudala et al.* 2002; *McFarquhar and Heymsfield* 1997; *Ivanova et al.* 2001). However, because of some uncertainties in the FSSP and 2D-C data for small particles, in this paper, the small ice particles ($D_i \leq 100$ µm) are included by extrapolating the parameterized spectra to smaller sizes. The large ice particles (D_i>575 µm) are included in the parameterization based on measurements using the 2D-

P probe which is capable of measuring sizes up to 6.4 mm (see section 2.2). However, this probe may not capture some of the particles near the 6.4 mm size end where the probe has a relatively small sample volume. Thus in this paper, the small and large particles are incorporated by integrating the parameterization from zero to infinity. More than 2040 30s averaged spectra were used for this parameterization. The comparison of this parameterization against observation will be discussed in section 6.

Table 1. Coefficient for ice particle spectra parameterization based on 30s averaged 2D-C and 2D-P measurements.

a_1 = 1.084E+001	a_2 = 1.1126E-003
b_1 = -2.0107E-001	b_2 = -6.38098E-002
c_1 = -1.2037E-002	c_2 = -3.37645E-003
d_1 = 2.011655E-001	d_2 = -2.1089E-001

6. COMPARISONS WITH MEASUREMNTS

Figure 8 shows comparisons of various parameters derived using measured 30s averaged ice spectra and the parameterization given in Eq. 12. The parameterization of the slope parameter agrees well with observation (panel a). Comparison of the parameterized ice concentration against observation is rather difficult since it depends on the limits of integration (panel b). When the size spectra parameterization is integrated from 125 µm to infinity, it agrees reasonably well with observation, but when it is integrated from zero to infinity (see Eq.3), the concentration of small ice particles is increased. The concentration of small ice particles could be very important for parameterization of ice microphysics, but as mentioned earlier the currently available probes do not measure them accurately. In the figure, the measured concentration with the FSSP probe is also shown for comparison. Therefore, in this paper, the small and large particles are included by integrating the parameterized spectra from zero to infinity as described in the previous sections. The parameterized ice deposition (panel c), riming (panel d), and terminal velocity (panel e) also agree well with observations. There is good agreement between the mass derived using the Heymsfield's coefficients and the mass measured using Nevzorov probe (panel f), but there are some discrepancies at low ice mixing ratios (see Fig. 3).

7. SUMMARY AND CONCLUSIONS

Using in-situ aircraft measurements of ice particle spectra in stratiform clouds during several field projects, the Meyers ice nucleation formula and the bulk ice microphysics scheme developed by *Kong and Yau* (997) based on the Meyers formula were tested. The ice concentration derived using the Meyers formula underestimates (overestimates) the concentration at warmer (colder) temperatures as compared to the 2D-C and 2D-P measurements. It was found that the ice mass or ice mixing ratio (q_i) derived assuming that ice particles are spheres with a density of pure ice significantly overestimates q_i as compared to both direct measurements using the Nevzorov probe and the one derived using Heymsfield's coefficients.

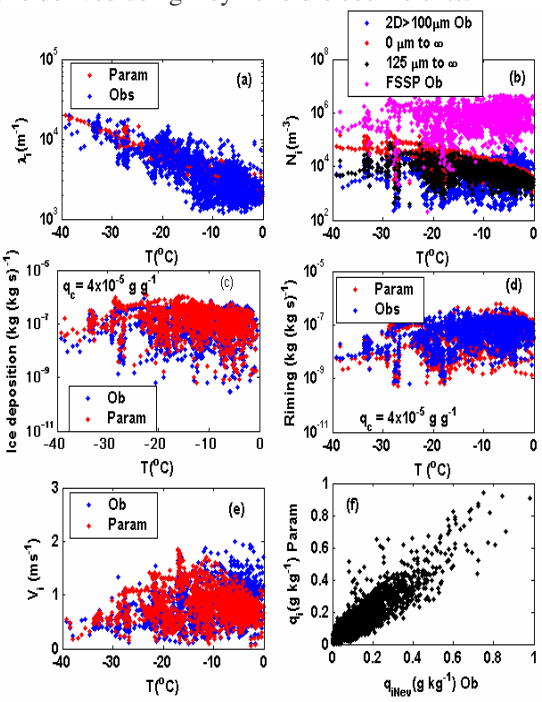

Figure 8. Comparisons of the parameterization against observations plotted against temperature (panels a-e) and the derived mixing ratio using the parameterized ice spectra plotted against observations.

The mass-weighted terminal velocity (V_i) derived using the KY scheme overestimates V_i for temperatures (T > -25 °C) as compared to values derived using the observed ice particle spectra and Heymsfield's $m-D_i$ relationships, although the same $m-v_i$ relationships for fall velocity is used in both schemes. Similarly, the ice deposition and riming rates are also overestimated at colder temperatures and underestimated at warmer temperatures as compared to the observations. The general tendency of KY is to increasing ice clouds at colder temperatures and decreasing ice clouds at warmer temperatures as compared to the observations based on the 2D-C and 2D-P measurements. A new parameterization of ice particle spectra in terms of temperature and q_i has been developed. It was shown that for a given q_i, both

λ_i and N_{io} increase with decreasing temperature. Decreasing λ_i with increasing temperature implies increasing aggregation with increasing temperature, and increasing N_{io} with decreasing temperature suggests the production of small ice particles. For a given temperature, λ_i (N_{io}) increases (decrease) with decreasing q_i , which suggests that increasing q_i is associated with an increase in both small ice particles and aggregation. The parameterization agrees reasonably well with observation and appears to overcome most of the temperature inconsistencies found between the model derived parameters and the observations. A more complete testing of the sensitivity of models to this new parameterization is required and efforts are underway to perform such a study.

8. ACKNOWLEDGEMENTS

This work was funded by the National Search and Rescue Secretariat, Transport Canada, the Panel on Energy Research and Development, the Canadian Climate Action Fund, the Natural Sciences and Engineering Research Council, as well as from U.S. sources including the Boeing Commercial Airplane Group, and the National Aeronautics and Space Administration, the Federal Aviation Administration. The data were collected using the Canadian National Research Council Convair-580 and the authors are grateful to their NRC colleagues for their assistance. Faisal Boudala also received funds from the National Science and Engineering Research Council (NSERC) and the Canadian Foundation for Climate and Atmospheric Sciences (CFCAS).

9. REFERENCES

Arnott, W. P., D. Mitchell, C. Schmitt, D. Kingsmill, D. Ivanova, and M. R. Poellot, 2000: Analysis of FSSP performance for measurement of small crystal spectra in cirrus. *Proceedings 13th Intl. Conf. on Clouds and Precipitation*, Reno Nevada, 14-18 August 2000, 191-193.

Boudala , 2004: Parameterization of ice crystal properties and liquid fraction in extra-tropical stratiform clouds, Dalhousie University Ph.D. thesis.

Boudala, F. S., A. G. Isaac, Q. Fu, and S. G. Cober , 2002, Parameterization of effective particle sizes for high latitude clouds. *Int. J. Climatology*, **22**, 1267-1284.

Benoit, R., M. Desgagné, P. Pellerin, S. Pellerin, S. Desjardins and Y. Chartier , 1997 : The Canadian MC2: a semi-Lagrangian, semi-implicit wide-band atmospheric model suited for fine-scale process studies and simulation. Mon. Wea. Rev., **125**, 238

Cooper, W. A. , 1986: Ice initiation in natural clouds. *Precipitation Enhancement-A Scientific Challenge, Meteor. Monogr.,* No. 21, Amer. Meteor. Soc., 29–32.

Curry, J. A., P. V. Hobbs, M. D. King, D. A. Randall, P. Minnis, G. A. Isaac, J. O. Pinto, T. Uttal, A. Bucholtz, D. G. Cripe, H. Gerber, C. W. Fairall, T. J. Garrett, J. Hudson, J. M. Intrieri, A. Jakob, T. Jensen, P. Lawson, D. L. Marcotte, L.Nguyen, P. Pilewskie, A. Rangno, A. Rogers, K. B. Strawbridge, F. P. J. Valero, A. G. Williams, and D. Wylie, 2000: FIRE Arctic Clouds Experiment. *Bull. Am. Meteorol. Soc.*, **81**, 5-29.

Ferrier, B. S., 1994: A double moment multiple phase four class bulk ice scheme. Part I: Description . *J. Atmos. Sci*., **51**, 249-290.

Field, P. R., R. Wood, and A. R. P. Brown, 2003: Ice particle interval times measured with FSSP. *J. Atmos. Oceanic Technol*., 20, 249-261.

Fletcher, N. H., 1962: Physics of Rain Clouds, Cambridge University Press, CSIRO.

Gardiner, B. A. and J. Hallett, 1985: Degradation of in cloud Forward Scattering Spectrometer Probe measurements in presence of ice particles. *J. Atmos. Oceanic Technol*., **13,**1152-1165.

Guan, H, S. G. Cober, G. A. Isaac, A. Tremblay, and A. Me´ thot, 2002: Comparison of three cloud forecast schemes with in situ aircraft measurements. Weather Forecasting. **17**. 1226-1235.

Gultepe, I., G. A. Isaac, and S. G. Cober, 2001: Ice crystal number concentration versus temperature *Int. J. Climatology***, 21,** 1281-1302**.**

Gultepe, I., G. A. Isaac, D. Hudak, R. Nissen, and J. W. Strapp, 2000: Dynamical and microphysical characteristics of Arctic clouds during BASE. *J. Climate*, **13**, 1225- 1254.

Heymsfield, A. J., 2003: Properties of tropical and midlatitude ice clouds particle ensembles. Part I: Median mass diameter and terminal velocities. *J. Atmos. Sci***., 60**, 2573-2591.

Heymsfield, A. J., A. Bansemer, P. R. Field, S. L. Durden, and J. L. Smith, 2002: Observations and parameterization of particle size distribution in deep tropical cirrus and stratiform precipitating clouds: Results from in situ observations in TRMM field campaigns. *J. Atmos. Sci*., **59**, 3457-3490.

Hallett, J. and S.C. Mossop. 1974: Production of secondary ice particles during the riming process. *Nature*, **249**, 26-28.

Isaac, G. A., S. G. Cober, J. W. Strapp, A.V.

Korolev, A. Tremblay, and D. L. Marcotte, 2001:Recent Canadian research on aircraft in-flight icing. *Canadian Aeronautics and Space Journal*, 47-3, 213-221.

Ivanova, D., D. L. Mitchell, W. P. Arnott, M. Poellot, 2001: A GCM parameterization for bimodal size spectra and ice mass removal rates in mid-latitude cirrus clouds. *Atmos. Res*., **59**, 89-113.

Knollenberg, R.G., 1970: The optical array: An alternative to scattering or extinction for airborne particle size determination. *J. Appl. Meteor*., **9**, 86-103.

Knollenberg, R. G. 1981 Techniques for probing cloud microstructure. In: *Clouds, their formation, Optical properties, and Effects*, P. V Hobbs, A. Deepak, Eds. Academic Press, 495 pp.

Korolev, A., G.A. Isaac, and J. Hallett, 2000: Ice particle habits in stratiform clouds. *Quart. J. Roy. Meteor. Soc*., **126**, 2873-2902.

Korolev, A. V., W. J. Strapp, and G. A. Isaac , 1998b: The Nevzorov airborne hot wire LWC-TWC probe: Principle of operation and performance. *J. Atmos. Oceanic Technol*., **15**, 1495-1510.

Korolev, A. V., W. J. Strapp, and G. A. Isaac , 1998a: Evaluation of accuracy of PMS optical array probe. *J. Atmos. Oceanic Technol*., **15**, 708-720.

Kong, F., and M.K. Yau, (1997), An Explicit Approach to Microphysics in MC2. *Atmosphere-Ocean*, 35, 257-291.

Licor LI-6262 CO2/HO2 Analyzer. Operating and Service Manual, 1996, Publication Number 9003-59, March, 1996, LI-COR Inc., Lincoln, Nebraska, USA.

Liou, K. N., 1986: Influence of cirrus clouds on weather and climate processes: A global perspective, *Mon. Weather Rev.*, **114**, 1167–1199.

McFarquhar, G. M. and A. J. Heymsfield, 1997: Parameterization of tropical cirrus ice crystal size distribution and implication for radiative transfer: Results from CEPEX. *J. Atmos. Sci.,* **54**, 2187-2200.

Meyers, M.P.; P.I. Demott and W.R. Cotton ,1992: New primary ice-nucleation parameterizations in an explicit cloud model. *J Appl. Meteorol*., **31**, 708-721.

Morrison, H, Curry, J. A., Shupe, M. D, and P. Zuidema, 2005: A new double-moment microphysics parameterization for application in cloud and climate models. Part II: Single-Column Modeling of Arctic Clouds. *J. Atmos. Sci.,* **62**, 1678-1693.

Morrison, H., Shupe, M. D., Curry, J. A., 2003. Modeling clouds observed at SHEBA using a bulk microphysics parameterization implemented into a single-column model. *J. Geophys. Res*. **108,** 10.1029/2002JD002906.

Pruppacher, H. R. and J. D. Klett, 1997: Microphysics of Clouds and Precipitation, Kluwer Academic Publisher.

Rotstayn, L. D., 1997: A physically based scheme for the treatment of stratiform clouds and precipitation in large-scale models Part I: Description and evaluation of the microphysical processes. *Q. J. R. Meteorol. Soc.,* **123**, 1227-1282.

Stephens, G. L., S. C. Tsay, and P. W. Flatau, 1990: The relevance of microphysical and radiative properties of cirrus clouds to climate and clime feedback, *J. Atmos. Sci.*, **47**, 1742–1753.

Vardiman, L., 1978: The generation of secondary ice particles in clouds by crystal collision. *J. Atmos. Sci.,* **35,** 2168-2180. Wilson, D.R. and

Ballard, S.P., 1999:A microphysically based precipitation scheme for the UK Meteorological Office Unified Model. *Q.J.R. Meteorol. Soc.*, **125**, 1607-1636.